Synchronization of Wind Farm Power System to Utility Grid under Voltage and Frequency Variations

Mouna Rekik*‡, Achraf Abdelkafi*, Lotfi Krichen*

*Department of Electrical Engineering, National School of Engineering, University of Sfax, 3038 Sfax, Tunisia

mouna_ing@hotmail.fr, achraf_abdelkafi@yahoo.fr, lotfi.krichen@enis.rnu.tn

‡Corresponding Author; Mouna REKIK, National Engineering School of Sfax, Control and Energy Management Laboratory (CEM_Lab) BP 1173, 3038, Sfax, Tunisia, Tel.: (+216) 74 274 418 / Fax: (+216) 74 275 595, mouna_ing@hotmail.fr

Received: 28.10.2014 Accepted: 20.12.2014

Abstract- The high penetration of micro-grid (MG) based on renewable distributed generators (DG) in the electrical network has brought about new issues on the stability and the transient operation of the grid. However, the disconnection and the reconnection of these local networks may give rise to undesired transient overcurrents and other damage that have to be avoided. In order to solve this problem, this paper presents a novel synchronization method for a DG grid connection. This synchronization method has been implemented in a grid-connected power converter that acts as an intelligent connection agent and adapts the magnitude, the frequency and the phase angle of the MG voltage at the point of common coupling (PCC) to be equal to those of the main voltage, despite the grid frequency and voltage variations. The system is simulated using MATLAB software and results are discussed in order to prove the performance and the robustness of this synchronization technique.

Keywords Micro-grid, Electrical network, Grid synchronization, Intelligent connection agent.

1. Introduction

Nowadays, the technological change, the environmental policies and the electricity markets, encourage the emergence of micro-grid (MG) for future intelligent power grids [1]. An MG is an energy system consisting of various distributed generating stations and loads capable of functioning independently from, or in parallel with, the main power grid [2]. Among the numerous benefits of MG is that it provides a closer proximity between energy generation and energy use, resulting in transmission reductions and efficiency increases. The MG also facilitates the high penetration of renewable distributed generation (DG) such as solar, wind power, small hydro, geothermal, to reduce CO2 emissions and fossil fuels consumption [3].

The MG can operate in two modes according to the state of the grid stability: The first one is the grid connected mode in order to endure increased energy demands and provide some additional services together with energy sale [4]. These additional services include: frequency and voltage adjustment, harmonic compensation, power backup, network stability, supplementary reserve and clearing load peaks… These auxiliary functions increase the strategic value of the MG decisively. The second one is the standalone mode in case of grid deficiency [5]. During this mode, the MG is disconnected immediately from the network and the DG is focused on providing emergency power supply to loads.

Connection and disconnection of the MG from the main grid cannot be guaranteed at any condition [6,7]. To achieve such a task and before the grid reconnection, the inverter output voltage must be synchronized with the utility voltage waveform. Moreover, because the grid voltage can occasionally be subjected to unpredicted and sudden perturbations such as phase change and/or voltage sag, such perturbations may result in a synchronization loss and, therefore, the inverter must be able to re-establish synchronization. If the MG systems are not properly synchronized, their connection to the utility network can lead, as a consequence, to grid instability or even failure [8].

So, to ensure a smooth reconnection to the main network when it is restored, a third mode called synchronization has become a need. Among the numerous published research works on islanded and parallel operation of micro-grids, there are only few studies, which specifically focus on the subject of MG resynchronization. For example, in [9], the authors proposed a synchronization method based on pitch angle controller, rotor flux adjustment and phase-locked loop (PLL) circuit for electrical network connection

of a doubly fed induction generator in a wind power generation system. However, this synchronization method is only used for a similar application and may not be applied for all types of MG. In [10], a grid synchronization method using a PLL algorithm based on the adaptive linear optimal filtering technique is proposed to control the disconnection, resynchronization, and the reconnection of the MG to the grid. A technique for the synchronization of electronic power converters taking into account only frequency variations is discussed in [11]. This technique is based on a hybrid structure and consists of a conventional synchronous-reference frame PLL and a feed forward frequency estimator loop. In [12], the authors proposed three solutions for this topic, based on the following advanced PLL topologies: a dual sogi PLL, a three phase enhanced PLL and a double synchronous reference frame PLL. All the methods proposed by [10-12] give a good synchronization between the network and the MG. However, they take into account only the grid frequency derivation which may arise during the synchronization mode. In [13], a voltage difference threshold was used to achieve the synchronization. A static switch was also applied to guarantee a transient free reconnection even in case the frequency and phase angles are not matched at the interconnection.

In this paper, a new synchronization technique between an MG and an electrical network was developed. This proposed technique was introduced in an intelligent voltage source inverter (IVSI) control. This IVSI is considered as a smart connection agent. In fact, the IVSI control analyzes the MG and the grid statements and provides the state of the different switches to reconnect the MG to the main grid at an optimum condition. With this proposed method, a reliable and deterministic synchronization under the condition of the fluctuating renewable outputs and rapid load change was achieved. This method synchronizes the components of the MG intelligently taking into account the simultaneous variation in the grid voltage or frequency at the point of common coupling (PCC). It is also able to re-establish synchronization when a grid voltage or frequency derivation may arise during the synchronization mode. The remaining of this paper is organized as follows. In Sect. 2, the studied system was presented. In Sect. 3, a brief outline of the MG modeling was provided with its respective control systems. Sect. 4 included the description of the proposed technique which is implemented in the IVSI to analyze the electrical network and the MG statements and ensure a robust synchronization between them. Finally, the obtained results when disconnecting and reconnecting the MG were presented and discussed in Sect. 5.

2. System Description

As shown in Fig. 1, the studied system may be subdivided into two crucial parts. The first one is the electrical network including the generation stations based on synchronous machines, the transmission lines operating at different voltage levels and external loads. The second one is the MG unit based on a wind farm made up of three wind turbine generators of a 2 MW variable-speed permanent magnet synchronous generator (PMSG). Each wind generator is connected to the DC bus through a PWM rectifier. The MG also comprises an IVSI, an RCL filter to reduce the harmonics generated by the IVSI converter and internal loads supplied by the wind farm stations. The entire MG is connected to the electric power system at the PCC through a Static Switch (SS). Unlike traditional switches, these switches provide faster transfer time, which ensures the uninterrupted operation of even the most sensitive electronic equipment [14,15]. The status of this switch as well as the operating mode of the IVSI depend on the reliability of the mains to meet the grid-interconnection standards, IEEE 1547 [7]. The functioning of this system is as follows. When the electric power system is stable, the IVSI operates in a grid connected mode. In this mode, the main objective of the IVSI is to track the grid voltage. The wind farm is controlled to supply the internal loads and to contribute in the system services by compensating the voltage and frequency fluctuations at the PCC. These fluctuations are compensated in order to keep them within the optimal operating threshold [16,17]. The excess of wind farm generated power serves to supply a portion of the external loads and the remainder is powered by the grid.

On the other hand, when a grid failure is detected, the MG logs out from the network by opening the static switch SS. Consequently, The IVSI output voltage and the grid voltage at PCC are no longer synchronized and the wind farm station focuses on providing emergency power to the internal loads. But when the grid deficiency is cleared, before reclosing the static switch SS, the MG voltage is synchronized in frequency, magnitude and phase-angle with the voltage of the utility network thanks to the proposed fast synchronization technique integrated in the IVSI control. The specific requirements and standard that need to be satisfied in the IVSI control to reconnect an MG to the network are shown in Table 1.

Table 1. Standards for IVSI control [7,16,17]

MG islanding	Maximum threshold of grid frequency Δf_m	$\pm 0.5\,Hz$
	Maximum threshold of grid voltage ΔV_m	$\pm 500\,V$
MG compensation	Optimum threshold of grid frequency Δf_{NA}	$\pm 0.1\,Hz$
	Optimum threshold of grid voltage ΔV_{NA}	$\pm 100\,V$
MG synchronization	Optimum threshold of frequency difference Δf_{syn}	$\pm 0.05 Hz$
	Optimum threshold of voltage difference ΔV_{syn}	$\pm 10\,V$
	Optimum threshold of phase angle difference $\Delta \theta_{syn}$	$1°$

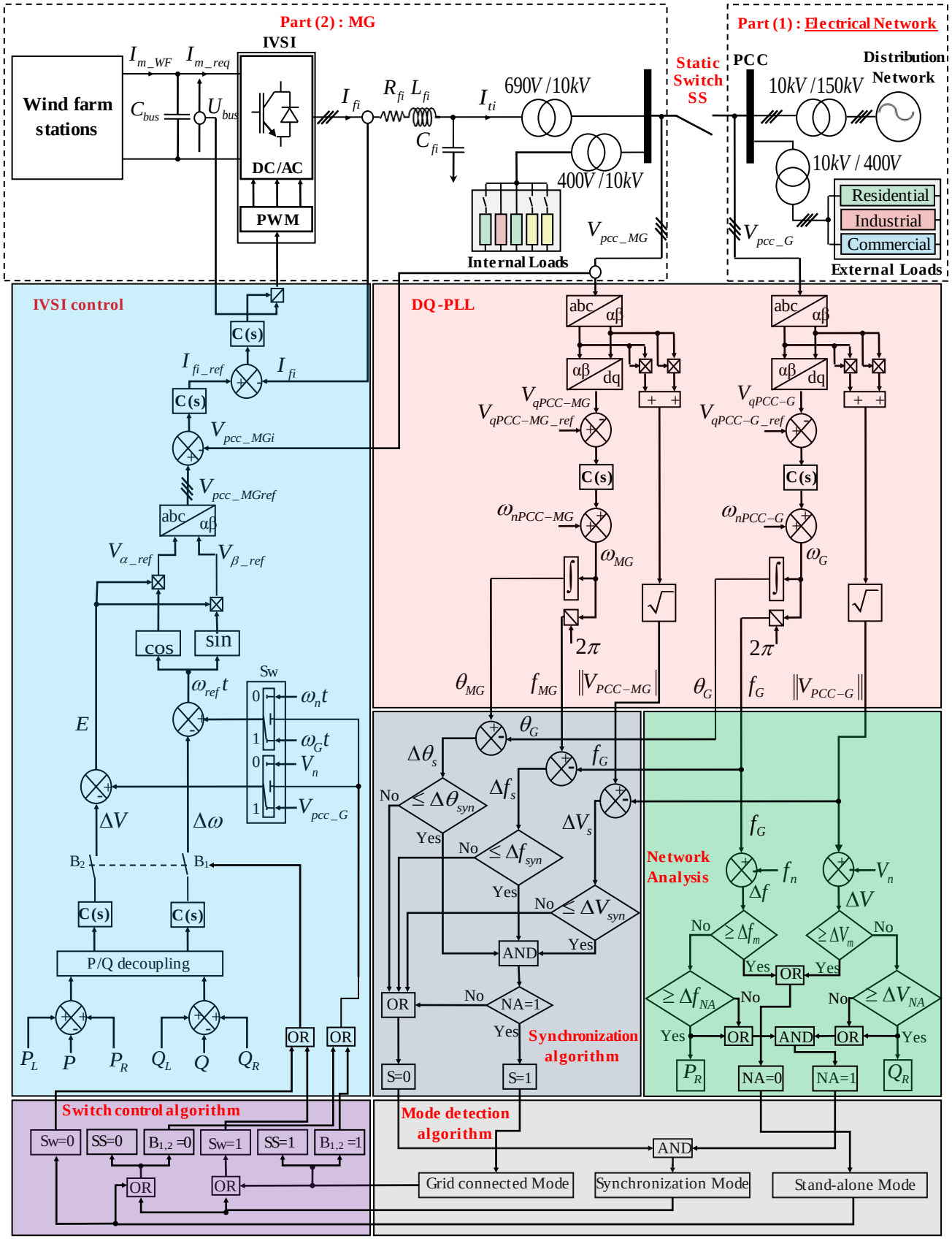

Fig. 1. Schematic blocks diagram of the proposed wind farm synchronization control to utility grid.

3. Utility Network Model and Stability Analysis

Electricity networks are made up of an energy infrastructure. Each network varies in size and structural components. However, they all share the same basic characteristics [18-19]. Its function is to deliver electric power from generating stations which consists generally of thermal and hydroelectric synchronous machines and to transport it to the consumption points through transmission lines operating at different voltage levels.

3.1. Salient Pole Synchronous Machine Modeling

Most of the electrical energy is produced currently by interconnecting Wound Rotor Synchronous Generators (WRSGs) power stations. WRSGs represent a preferred choice in high-power drive applications in the range of a few MWs to 100s of MW. This is due to its various advantages like robustness, high-voltage design economy and power factor control capability. They are also playing an important role to ensure the network stability. In fact, they impose the system frequency and produce or absorb reactive power required to regulate voltages at any bus of the grid [20]. In this paper, the studied WRSG was modeled in d-q axes frame under the following equations [21, 22]:

$$\begin{cases} V_d = -r_s i_d + l_q \omega_{ep} i_q - M_{sQ} \omega_{ep} i_Q - l_d \dfrac{di_d}{dt} + M_{sf} \dfrac{di_f}{dt} + M_{sD} \dfrac{di_D}{dt} \\ V_q = -r_s i_q - l_d \omega_{ep} i_d + M_{sf} \omega_{ep} i_f + M_{sD} \omega_{ep} i_D - l_q \dfrac{di_q}{dt} + M_{sQ} \dfrac{di_Q}{dt} \\ V_f = r_f i_f + l_f \dfrac{di_f}{dt} - M_{sf} \dfrac{di_d}{dt} + M_{fD} \dfrac{di_D}{dt} \\ 0 = r_D i_D + l_D \dfrac{di_D}{dt} + M_{fD} \dfrac{di_f}{dt} - M_{sD} \dfrac{di_d}{dt} \\ 0 = r_Q i_Q + l_Q \dfrac{di_Q}{dt} - M_{sQ} \dfrac{di_q}{dt} \\ J \dfrac{d\Omega_{ep}}{dt} = \mathrm{T}_e - \mathrm{T}_m \end{cases} \quad (1)$$

T_e is the electromagnetic torque based on the current machine, it is given by

$$\mathrm{T}_e = \frac{3}{2} n_p (\phi_d \, \mathrm{i}_q - \phi_q \, \mathrm{i}_d) \quad (2)$$

With ϕ_d and ϕ_q are the direct and transverse stator leakage flux. The following relationships can be written [23]:

$$\begin{bmatrix} \phi_d \\ \phi_q \end{bmatrix} = \begin{bmatrix} -l_d & 0 & M_{sf} & M_{sD} & 0 \\ 0 & -l_q & 0 & 0 & M_{sQ} \end{bmatrix} \begin{bmatrix} i_d \\ i_q \\ i_f \\ i_D \\ i_Q \end{bmatrix} \quad (3)$$

3.2. Loads Modeling

In order to model the views loads departures distribution, the exponent model expressed by the following equations is adapted [19]:

$$P_L = P_0 \left(\frac{V_L}{V_0} \right)^{\alpha} \quad (4)$$

$$Q_L = Q_0 \left(\frac{V_L}{V_0} \right)^{\beta} \quad (5)$$

Where V_0 is the reference voltage, P_0 and Q_0 are active and reactive consumed powers under this voltage. α and β designate the type of load [24].

The sudden and random variations of power levels required by the external loads connected at the PCC may cause significant drifts in grid voltage and frequency at the same consumption points. The absence of a robust control at the renewable DG level output can also cause problems with power quality (both voltage and frequency). According to [25], the network can operate in two situations: The first one is the state of stability when fluctuations in frequency and voltage are within the stability range mentioned in Table 1. And the second one is the instability sate, when these fluctuations exceed these limits. In this paper, a third state was added which is the state of optimum stability. In that, the grid voltage and frequency fluctuations are compensated into an optimum threshold of stability thanks to the proposed command applied to the wind turbine farm during the grid connected mode.

4. Wind Farm Stability Analysis

This section presents the studied wind farm which is composed of three turbines based on a PMSG with its own control schemes. This wind farm is used not only to supply islanded loads, but also to participate in the system services. In fact, it can produce smooth power and ensure the balance between power generation and consumption at different wind conditions without adding any storage systems, thanks to the novel proposed control strategy shown in Fig.2.

4.1. Wind Turbine Generator Model

The wind turbine serves to capture the wind's kinetic energy in order to convert it into a mechanical torque rotatable rotor blades. The tip-speed ratio is obtained by the following expression [26]:

$$\lambda = \frac{\Omega_t R}{\nu} \quad 6)$$

The extracted mechanical power by the variable wind turbine speed can be expressed in the following way [26]:

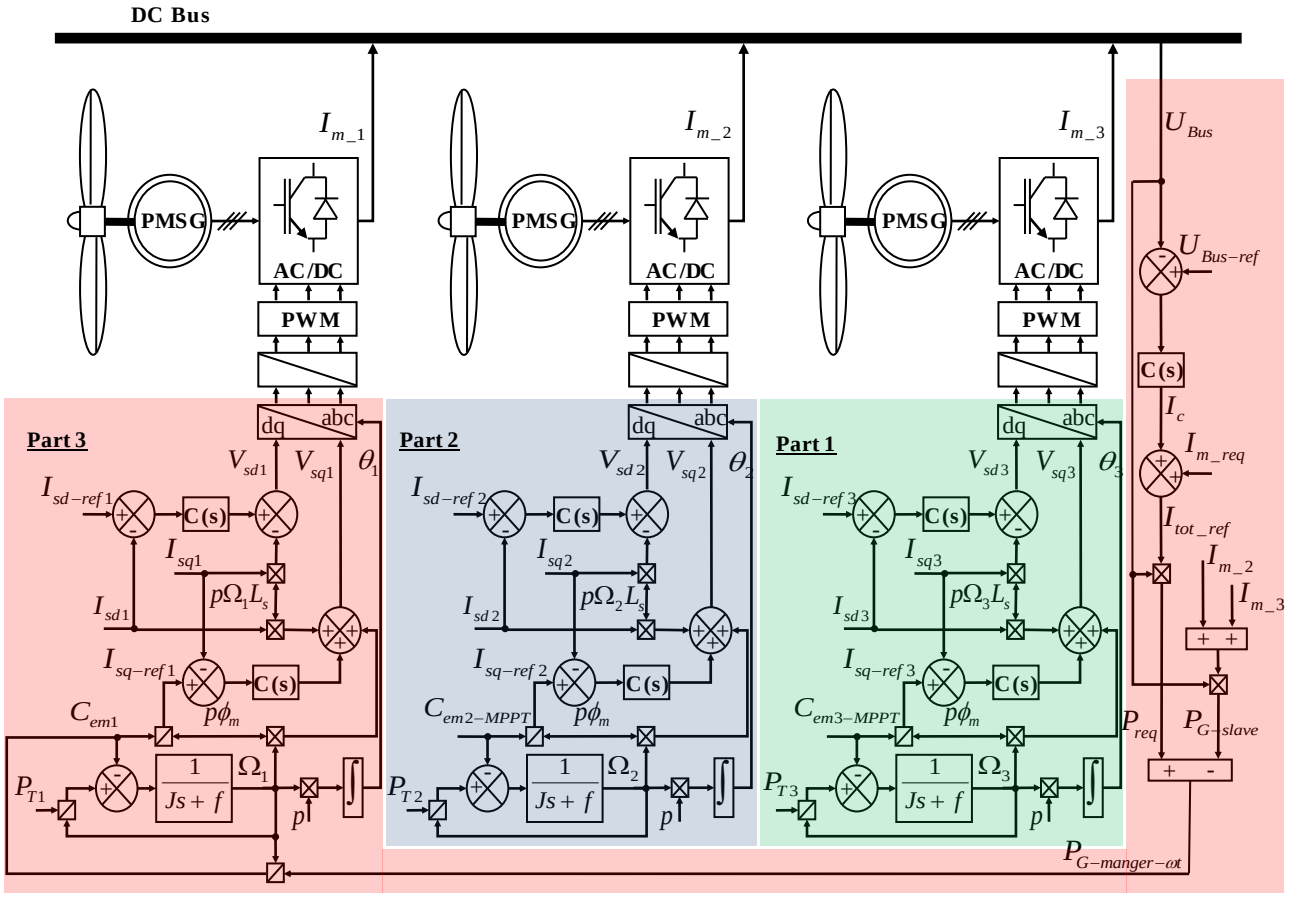

Fig. 2. Wind farm control strategy

$$P_m = \frac{1}{2} C_p . \rho . S . v^3 \tag{7}$$

The fundamental dynamics equation to determine the evolution of the PMSG mechanical speed and the mechanical torque expression on the wind turbine rotor are defined by [27]:

$$J \frac{d\Omega}{dt} = C_m - C_{em} \tag{8}$$

$$C_m = \frac{P_m}{\Omega} \tag{9}$$

Considering that the studied PMSG is a machine with smooth poles $\left(L_d = L_q = L_s\right)$ and surface mount-type radial magnet, the current and the torque of the PMSG can be modulated in the d-q frame by the following equations [28]:

$$\begin{bmatrix} \frac{dI_{sd}}{dt} \\ \frac{dI_{sq}}{dt} \end{bmatrix} = \begin{bmatrix} -\frac{R_S}{L_d} & p\,\Omega \\ -\frac{R_s}{L_q} & p\,\Omega \end{bmatrix} \begin{bmatrix} I_{sd} \\ I_{sq} \end{bmatrix} + \begin{bmatrix} \frac{V_{sd}}{L_d} \\ \frac{V_{sq} - p\,\Omega\,\phi_m}{L_q} \end{bmatrix} \tag{10}$$

$$C_{em} = p . \phi_m . I_{sq} \tag{11}$$

4.2. Wind Farm Control

The wind is known to be very unpredictable and fluctuating, which makes its turbine unable to meet the instantaneous demands and to participate in the system services [29,30]. As a result, this type of source behaves as passive generators and will pose problems for the energy system managers. Therefore, in order to eliminate these fluctuations and ensure a balance between consumed and generated powers, the wind turbine should produce nothing more or less than, the required energy. Various approaches have added storage systems to solve this problem [31,32]. This paper proposes a novel solution without the addition of any kind of storage systems to ensure the balance between wind turbine energy production and consumption and keep a soluble generation without fluctuation at any wind condition. This proposed control strategy is illustrated in Fig.2. The wind farm is divided into two groups of wind turbines which are interconnected in a specific way. The first group contains the slaves wind turbines and the second contains the smart manager wind turbine. The slaves wind turbines operate only in MPPT to meet the greatest amounts of loads and to

participate in the system services. But the smart manager wind turbine is responsible for ensuring a smooth generated power without any fluctuation caused by the stochastic winds on the one hand and for guaranteeing instantaneous equilibrium between the slaves wind turbines generated powers and consumers' required power, on the other. It is also responsible for adjusting the bus voltage in order to make it constant at any wind or demand conditions. The principle of the slaves wind turbines controls, shown schematically in parts 1 and 2 of Fig.2, is the same. The slaves wind turbine-side converter controls the generator torque to get a variable speed operation with the MPPT regulator. To achieve a maximum torque control of the PMSG and minimize resistive losses, the reference direct stator currents, $I_{sd-ref\,2,3}$ are set to zero. Thus, the generator torque may be controlled directly by the quadrature current component. The required d-q axis voltages of the rectifier are achieved by adding the two proportional and integral (PI) current controllers output with the compensation terms. The control needs the measurement of the rotor position, the stator currents and the DC bus voltage. After Park transformation of the d-q rectifier voltage, Pulse Width Modulation (PWM) is applied to generate the switching signals. Part 3 of Fig.2 illustrates the control applied to the smart manager wind turbine. The principle of this control consists of applying a reference torque in the PMSG equivalent to the required torque. In fact, the smart manager wind turbine receives information about the slaves wind turbines generated powers instantaneously and the required power for loads and system services simultaneously. Then, it calculates the difference between them. The imposed reference torque on the manager control generator is finally obtained by dividing the sum of this calculated power and losses by the rotor mechanical speed of the manager PMSG. Consequently, the manager wind turbine generates a torque similar to the asked torque to ensure the balance between production and consumption and to guarantee continued voltage at DC bus without adding any type of storage systems.

5. MG and Grid Synchronization

One of the most important issues to be solved before plugging the MG to the grid is to perform a smooth and accurate synchronization with the mains voltage. As shown in Fig. 1, the synchronization technique is divided into six main blocks: DQ-PLL, network analysis, synchronization algorithm, mode detection, switch control and IVSI control. The proposed synchronizing control operates using the communication between these different blocks. At first, the grid voltage V_{pcc_G} magnitude, phase and frequency and the same characteristics of the MG voltage V_{pcc_MG} at the PCC point are calculated by two DQ- Phase Locked Loops (DQ-PLL). Each one consists of Clarke's transformation, Park's transformation, a PI regulator and an integrator. The schematic of both DQ-PLL is shown in Fig. 1. In that, the DQ voltage components are derived from equation (12) using park's transformation. Where $\hat{\theta}_j$ represents the estimated voltage vector phase angle and $\|V_j\|$ is the source voltage module of the network or MG $j \in \{PCC\_G, PCC\_MG\}$.

$$\begin{bmatrix} V_{dj}(\theta) \\ V_{qj}(\theta) \end{bmatrix} = \begin{bmatrix} \cos\hat{\theta}_j & \sin\hat{\theta}_j \\ -\sin\hat{\theta}_j & \cos\hat{\theta}_j \end{bmatrix} \begin{bmatrix} V_{\alpha j} \\ V_{\beta j} \end{bmatrix} = \|V_j\| \begin{bmatrix} \cos(\theta_j - \hat{\theta}_j) \\ \sin(\theta_j - \hat{\theta}_j) \end{bmatrix} \quad (12)$$

Assuming that the angle $(\theta_j - \hat{\theta}_j)$ is very small, one can write:

$$V_{qj}(\theta) = \|V_j\|(\theta_j - \hat{\theta}_j) \quad (13)$$

The lock is achieved by setting the error $(\theta_j - \hat{\theta}_j)$ to zero. In this case, $V_{dj} = V_j$ and $V_{qj} = 0$. Thus, this PLL uses a PI regulator to adjust the error between V_{qj} and $V_{qj\_ref} = 0$. Consequently, at the regulator output we obtain the angular frequency variation $\Delta\omega_j$ which is added to the nominal angle frequency ω_{nj}. Afterwards, the angle estimation $\hat{\theta}_j$ is determined through the integration of this summation.

After the modules, frequencies and phase estimation at PCC point, the block "network analysis" of Fig.1 receives the output of the DQ-PLL network side as an input. This block analyzes the network stability and instability states in PCC. It measures the grid voltage and frequency at each instant and compares them with the stability thresholds mentioned in Table 1. Indeed, if "$\left(\Delta f \geq \Delta f_m\right)$ or $\left(\Delta V \geq \Delta V_m\right)$", the network in this case is broken down and unstable. Hence, the "network analysis" block sends a status signal $NA = 0$ as an output causing the opening of the static switch SS in order to disconnect the MG from the network, and the opening of B_{12} to stop the control of the power transferred between them. This is the stand-alone mode. In this case, the MG based on the wind farm ensures a steady supply for internal loads by imposing its own frequency and voltage (switch SW_{12} is at position "0").

But, when the default disappears and the network is back to its stability meaning "$(\Delta f < \Delta f_m)$ and $(\Delta V < \Delta V_m)$", the network analysis signal NA is turned immediately to "1" meaning that there is no islanding defect. In this case, the grid voltage and frequency may fall into two margins: the optimum margin or the regulation

one. If "$(\Delta f < \Delta f_{NA})$ and $(\Delta V < \Delta V_{NA})$", the grid in this state operates in its optimum stability, because the grid voltage and frequency variations are into the margin of efficient functioning "$\left(\pm \Delta V_{NA}, \pm \Delta f_{NA}\right)$" respectively.

Else, if "$(\Delta f_m > \Delta f \geq \Delta f_{NA})$ or $(\Delta V_m > \Delta V \geq \Delta V_{NA})$", the electrical network is stable but it is not in the optimum of stability because there are still some fluctuations in the voltage or frequency which are not dangerous but on the long-run may cause harmful consequences to loads. These fluctuations are eliminated, when the MG is connected to the grid, through the absorption or the injection of active and reactive powers P_R, Q_R into the electrical network at the PCC point.

So, when $NA=1$ the MG based on the wind farm prepares the reconnection to the network. Several actions will be carried out simultaneously to ensure this reconnection. The "Synchronization algorithm" block of Fig.1 analyzes the state of MG voltage side V_{pcc_MG} relative to the state of the network voltage side V_{pcc_G}. Indeed, it receives as input both of the PLL outputs and it computes the difference between the modules, the frequencies and the phases of the network and the MG at each instant. Then, it compares them with the tolerable limits of synchronization "$(\Delta f_{syn}, \Delta V_{syn}$ and $\Delta\theta_{syn})$" indicated in Table 1. This algorithm provides a signal S as output which can be equal to "1" only when both of voltage V_{pcc_MG} and V_{pcc_G} are synchronized in amplitude, frequency and phase and the MG is able to be reconnected to the network again. Otherwise, S may be equal to "0" in the two following cases: The first one is during the standalone mode meaning $NA=0$, and the second one is when "$\left(NA=1\right)$ and $\left[\left(\Delta f_s \geq \Delta f_{syn}\right)\right.$ or $\left(\Delta V_s \geq \Delta V_{syn}\right)$ or $\left.\left(\Delta\theta_s \geq \Delta\theta_{syn}\right)\right]$" means that, the grid is stable but the voltages V_{pcc_MG} and V_{pcc_G} are not yet synchronous in module, frequency and phase; that is the synchronization mode. In this case, in order to ensure the synchronization between these two voltages, the static switch SS is still open and the MG is also still disconnected from the network waiting for voltages synchronization. In addition, the "IVSI control" block shown in Fig.1 receives the amplitude and the frequency of the actual network voltage V_{pcc_G}. Then, the switcher SW_{12} changes from position "0" to position "1" to impose these parameters as references in the MG inverter control. In this situation, the MG reference voltage $V_{pcc\_MG\ ref}$ becomes equal to V_{pcc_G}. After that, the "IVSI control" adjusts, using PI regulators, V_{pcc_MG} with $V_{pcc\_MG\ ref}$ until the difference of amplitude, frequency and phase between these two voltages becomes less than the allowable synchronization threshold $(\Delta f_{syn}, \Delta V_{syn}$ and $\Delta\theta_{syn})$. In this situation, V_{pcc_MG} and V_{pcc_G} become synchronized, and the signal S turns immediately to "1" which simultaneously causes the closing of the static switch SS and the reconnection of the MG to the grid. Therefore, the MG becomes in the grid connected mode.

6. Simulation Results

Simulations of the MG based on this wind farm and the applied control strategies to synchronize this MG to the grid despite the presence of voltage and frequency fluctuations have been carried out. The parameters of the wind turbine and the generator used in this research are summarized in Table 2. In order to evaluate the dynamic responses of the proposed synchronization control strategy maintaining the management of the wind farm energy, three wind profiles represented in Fig. 3.a. on a period of 100 s are applied.

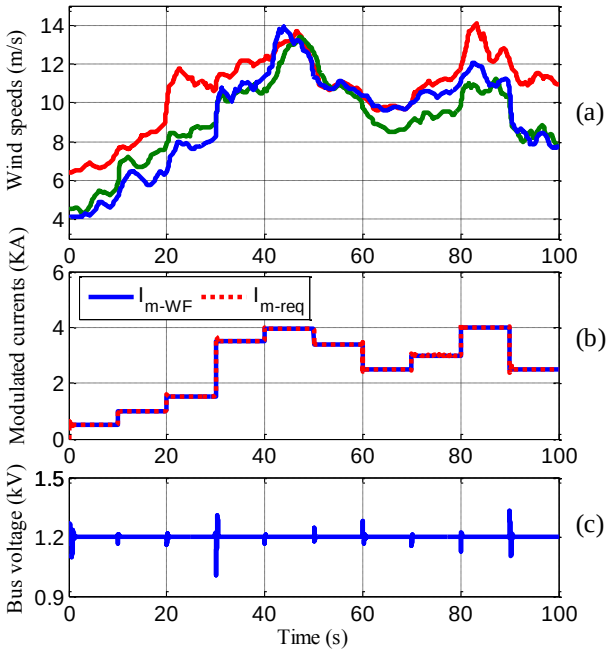

Fig. 3. Wind speeds (a) - Currents at DC bus level (b) and DC-bus voltage (c).

The red curve shows the wind speed waveform for the manager wind turbine and the curves in blue and green represent the wind speed waveforms for the slaves wind turbines. Fig. 3.b. shows the two currents on the DC bus. This figure demonstrates that the current provided by the wind farm generators and the one absorbed by the loads and the grid are equal. The slaves wind turbines operating in MPPT produce the maximum current possible at each wind value in order to supply the maximum of loads and participate in the system services. At the same time, the smart manager wind turbine provides the difference between the slaves wind turbines current and the required

current by the loads, grid and losses in order to ensure both a smooth wind farm generation without any fluctuation, and a bus voltage regulation without adding any type of storage system. The balance between the generated wind farm current and the required current on the DC bus level enables us to obtain a constant DC bus voltage at 1200 V as shown in Fig. 3.c. which proves the efficiency of the control strategy applied to the wind farm.

In order to analyze the stability/ instability states of the network at the PCC, the "network analysis" block receives the frequency and the module of the grid voltage in PCC as input presented by the red curves of Fig.4.a and.4.b, respectively. Then, it generates an output signal NA presented in Fig.4.c. Within the [0, 20 s], [40, 60 s] and [80, 100 s] intervals the grid is in its optimum stability because the voltage and the frequency fluctuations are into the margin of the efficient operation "$(10kV \pm \Delta V_{NA}$, $50Hz \pm \Delta f_{NA})$". In this case, the signal NA is equal to "1" (no faults detection). During the [20, 30 s] and [60, 70 s] periods, the grid is also stable, so NA is equal to "1". However, it is not at the optimum of its stability because the main voltage and frequency fluctuations are not included within the optimum stability ranges. In this case, the MG will be introduced to minimize these variations by extracting or injecting active and reactive powers into the electrical network. The zooms presented in Fig.4.a and .4.b clearly show the voltage and frequency before and after regulation by MG. It is noticeable that during the [20, 30 s] and [60, 70 s] periods, the grid voltage and frequency variations after regulation presented by the blue curves are well minimized and become into the desired range which proves the capability of the proposed MG to participate in the system services.

For the [30, 40 s] and [70, 80 s] periods, the grid is unstable because the main voltage and frequency fluctuations exceed the maximum thresholds. In this case, NA is equal to zero. These fluctuations can have a bad impact on the MG electrical equipments and personnel, so the MG cannot be introduced to regulate the grid voltage and frequency fluctuations. It should be isolated from the network to be secure from these strong variations. During these periods, the MG based on wind farm ensures the steady supply for internal loads by imposing its own frequency and voltage. Yet, the MG is still disconnected waiting for the defaults to be cleared to be able to reconnect to the electrical network.

Fig.5.d shows the output signal S of "synchronization algorithm" block which analyzes the state of the MG voltage side V_{pcc_MG} relative to the state of the network voltage side V_{pcc_G}. As shown in Fig.5.a, 5.b and 5.c, the grid and the MG voltages during the [0 30s], [40.05 70s] and [80.07 100s] periods are synchronized in modules, frequencies and phases and in this case, the signal S is equal to one. For the [30, 40 s] and [70, 80 s] periods, the "network analysis" block detects a default on the grid and thus($NA=0$).In this situation, the MG disconnects immediately from the network and the grid and the MG voltages are not yet synchronized so S becomes equal to zero. In [40, 40.05 s] and [80, 80.07 s], the grid is recovered again, NA returns to one (no grid defaults detection), but the grid and the MG voltages are not yet synchronized in modules, frequencies and phases. So S remains equal to zero.

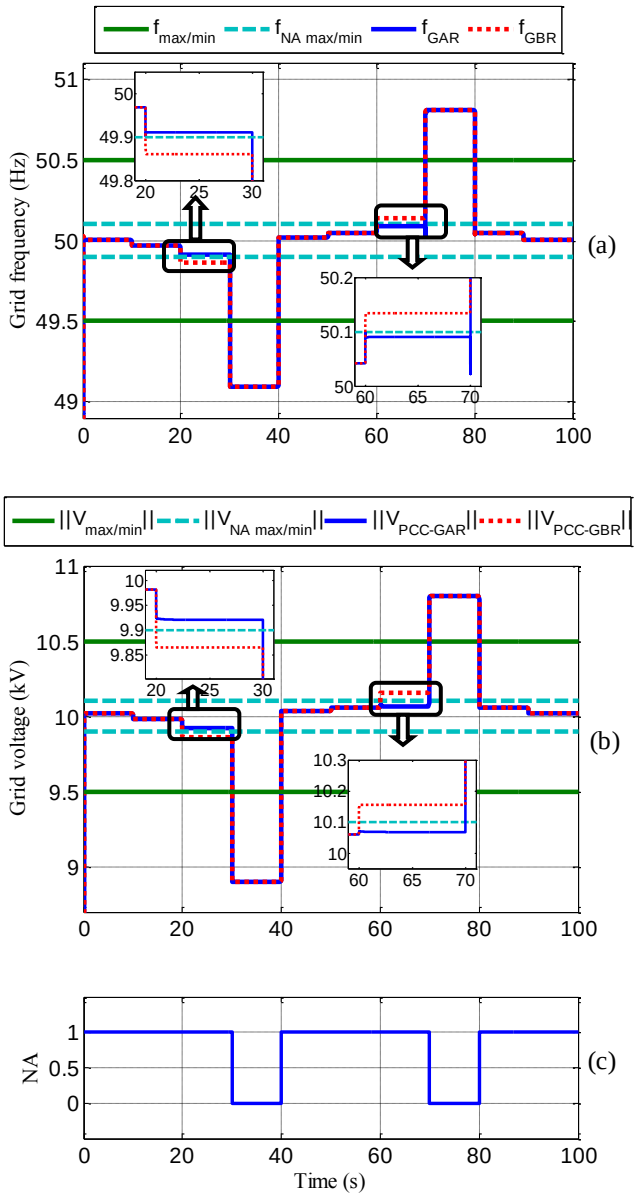

Fig. 4. Grid frequency at PCC before and after regulation (a) - Grid voltage at PCC before and after regulation (b) and response of the "network analysis" block (c).

Fig.6. shows the interactive operating modes of the MG system. These modes are automatically detected according to the states of "synchronization algorithm" block output signal S and to the states of the "network analysis" block output signal NA. Fig.6.a illustrates the grid connected mode. This mode is distinguished when $S=1$ (the grid and MG voltages are synchronized at PCC). Fig.6.b represents the standalone mode. The MG operates in this mode when a grid fault is detected by the

"network analysis" block ($NA = 0$). Fig.6.c represents the synchronization mode. This mode is detected when the grid is recovered again $NA = 1$ (no grid faults detection) and $S = 0$ (the grid and MG voltage are not yet synchronized in modules, frequencies and phases).

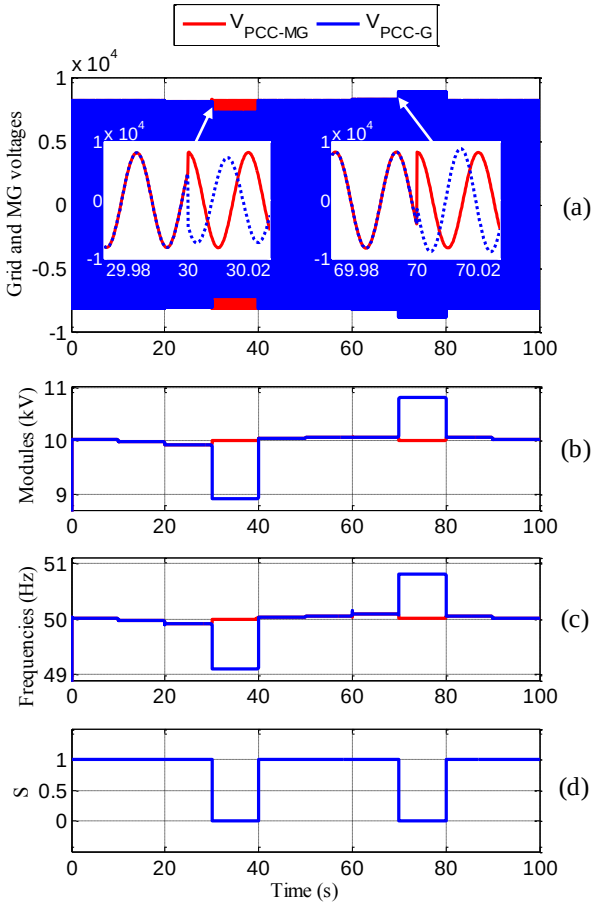

Fig. 5. MG and grid voltages profiles at PCC (a) - MG and grid modules (b) – MG and grid frequencies (c) and response of the "synchronization algorithm" block (d).

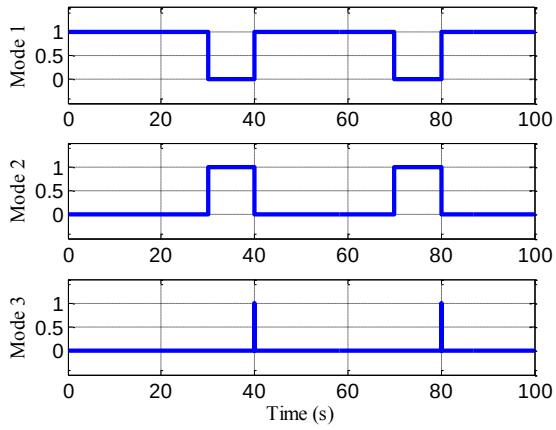

Fig. 6. Different operating modes of the MG.

Fig .7 represents the reaction of SW_{12}, B_{12} and SS under different operation modes. During the grid connected mode, the MG is connected to the grid in PCC so the static switch SS is closed ($SS = 1$) and the switcher SW_{12} takes the position of "1" to impose the grid voltage and frequency as reference to the MG inverter. The interrupter B_{12} works only during this mode and in the case of the grid voltage and frequency regulation. Indeed, during the [20 30s] and [60 70s] periods, B_{12} is closed ($B_{12} = 1$) to reduce voltage and frequency fluctuations by adopting the power supplied by the inverter to the total powers consumed by the load and the grid $(P_L + P_R)$ and $(Q_L + Q_R)$. During the stand alone mode, the MG is disconnected from the grid. The static switch SS is open ($SS = 0$), B_{12} is also open ($B_{12} = 0$) because there is no power transfer between the grid and the MG. At the same time, SW_{12} is changed to "0" to impose the wind farm frequency and voltage as a reference to its own inverter control. During the synchronization mode, SS and B_{12} are still open. But as shown in the zoom of Fig.7, the switcher SW_{12} changes to the state of "1" to impose the grid voltage and frequency as reference to the MG inverter so that the "IVSI control" block adjust the MG voltage to that of the grid at PCC until they are synchronized. Now, the static switch SS is closed and the MG reconnects again to the electrical network.

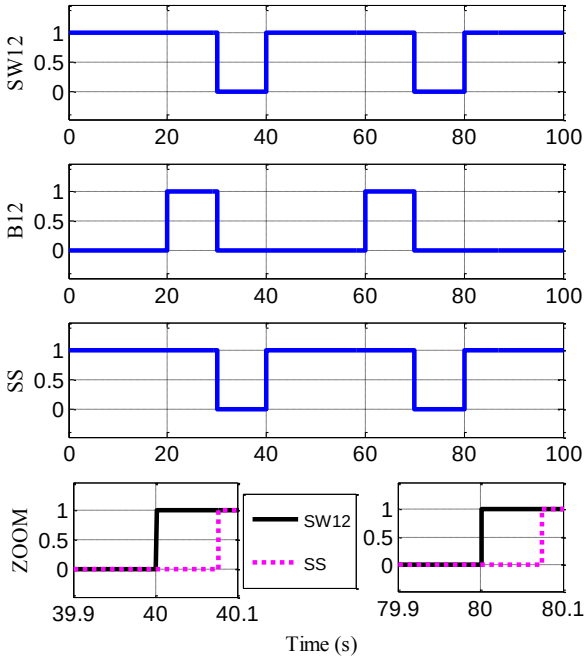

Fig. 7. Response of the "Switch control algorithm" block.

The behavior of the MG and the grid voltages V_j and phases θ_j during the synchronization mode are described in Fig.8. It is clearly noticeable that when the grid is recovered at t=40s and t=80s, the MG prepares to be reconnected to the network. It adjusts its own voltage and

phase, using the proposed control strategy to be synchronous with those of the grid.

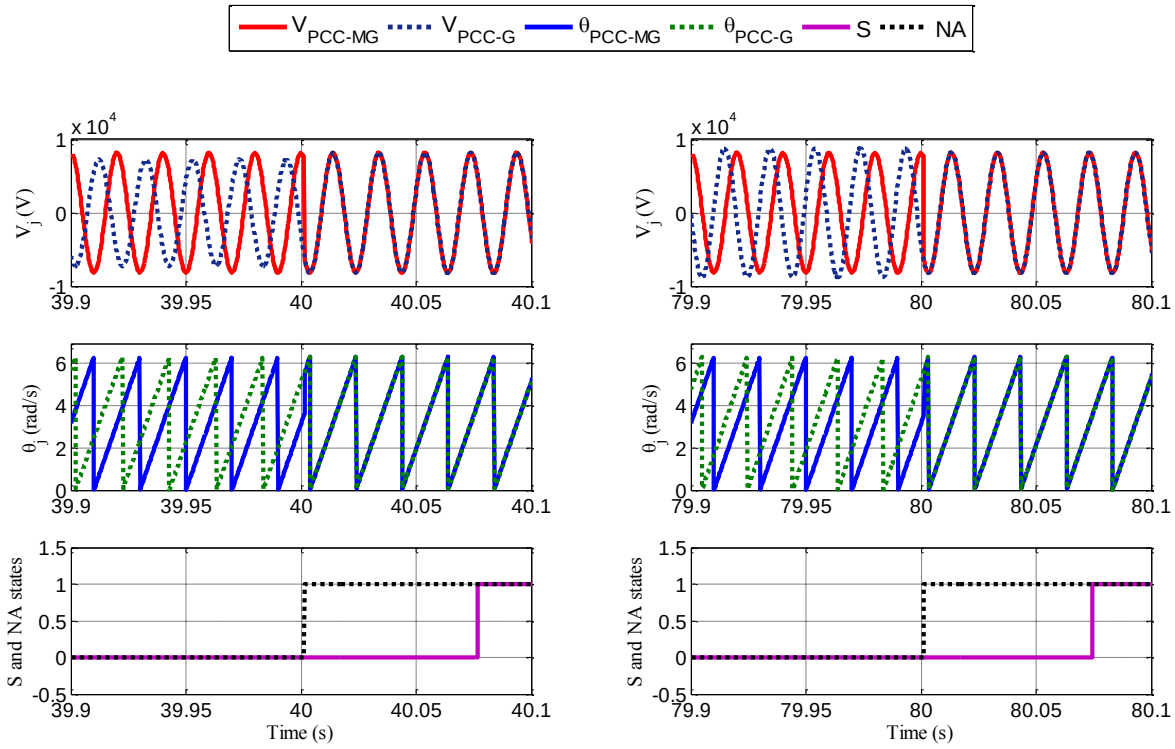

ZOOM at t=40 s ZOOM at t=80 s

Fig. 8. MG and grid synchronization at t=40s and t=80s.

In this case, the signal S turns immediately to one and the MG can be connected safely to the network. It can also be remarked that the grid and the MG synchronization is very fast. It might be ensured that it takes into account the variations of the grid voltage and frequency at PCC which may arise during the synchronization mode. This obviously proves the effectiveness and the robustness of the applied control strategy

Table 2. Studied wind turbine parameters

Wind turbine	Number of blades	3
	R	$41\ m$
	ρ	$1.22 Kgm^{-3}$
	v_N	$11.2\ m/s$
PMSG	Nominal power	$2\,MW$
	p	60
	R_s	$8.278 m\Omega$
	L_s	$1.285\ mH$
	ϕ_m	$4.813\ V(rad\ s^{-1})^{-1}$
	J	$10^5\ kgm^{-2}$
	Ω_N	$5.23\ rad/s$
DC bus	C_{bus}	$2200\ \mu F$

7. Conclusion

In this paper, a novel synchronization technique was proposed for MG based on wind farm to the utility grid, despite the grid frequency and voltage variations. The structure of this technique involves different interconnected control blocks. These are namely the "network analysis" block which is responsible for detecting the electrical network instability; the "synchronization algorithm" block which analyzes the state of the MG relative to the network at PCC; the "mode detection" block that detects the MG operation modes based on the previous blocks output signals; the "switch control" block which orders the various switches according to the detected mode and the "IVSI control" block which implements all these in the grid-connected power converter to act as an intelligent connection agent. The obtained results for the various grid voltage and frequency conditions demonstrate that the proposed synchronization technique gives a smooth and fast synchronization as well as a better robustness which allows the MG system to reclose quickly again to its normal operating after the grid default disappears.

References

[1] M. Xia, X. Li, "Design and Implementation of a High Quality Power Supply Scheme for Distributed

Generation in a Micro-Grid", *Energies*, vol. 6, pp. 4924-4944, 2013.

[2] N. Pogaku, M. Prodanovic, T. Green, "Modeling, Analysis and Testing of Autonomous Operation of an Inverter-Based Microgrid," *IEEE Trans. Power Electron*, vol. 22, pp. 613-625, 2007.

[3] A.A. Bhuiyan, A.K.M.S. Islam, A.I. Alam, "Application of Wind Resource Assessment (WEA) tool: A case study in Kuakata, Bangladesh," *International Journal of Renewable Energy Research*, vol. 1, pp.83-90, 2011.

[4] B. Singh, "Introduction to FACTS Controllers in Wind Power Farms: A Technological Review," *International Journal of Renewable Energy Research*, vol. 2, pp. 166-212, 2012.

[5] Q. Jiang, M. Xue, G. Geng, "Energy Management of Microgrid in Grid-Connected and Stand-Alone Modes," *IEEE Trans. Power Syst*, Vol. 28, pp. 3380-3389, 2013.

[6] J.C. Hernández, J. De la Cruz, B. Ogayar, "Electrical protection for the grid-interconnection of photovoltaic-distributed generation," *Electr. Power Syst. Res*, vol. 89, pp. 85-99, 2012.

[7] IEEE Standard 1547-2003, IEEE Standard for Interconnecting Distributed Resources with Electric Power Systems, *IEEE: Piscataway, NJ, USA*, 2003.

[8] L.C. Gross, L.S. Anderson, R.C. Young, Avoid generator and system damage due to a slow synchronizing breaker, *Wisconsin Electric Power Company and Schweitzer Engineering Laboratories*, USA, 1997.

[9] A.G. Abo-Khalil, "Synchronization of DFIG output voltage to utility grid in wind power system," *Renew. Energy*, vol. 44, pp. 193-198, 2012.

[10] Y. Han, L. Xu, M.M. Khan, G. Yao, L.D. Zhou, C. Chen, "A novel synchronization scheme for grid-connected converters by using adaptive linear optimal filter based PLL (ALOF–PLL) ," *Simul. Model. Pract. Th*, vol. 17, pp. 1299-1345, 2009.

[11] B.I. Rani, C.K. Aravind, G.S. Ilango, C. Nagamani, "A three phase PLL with a dynamic feed forward frequency estimator for synchronization of grid connected converters under wide frequency variations," *Elec. Power Energy Syst*, vol. 41, pp. 63-70, 2012.

[12] S. Golestan, M. Monfared, F.D. Freijedo, J.M. Guerrero, "Advantages and Challenges of a Type-3 PLL," *IEEE Trans. Power Electron*, vol. 28, pp. 4985-4997, 2013.

[13] R.H. Lasseter, P. Piagi, Control and design of microgrid components, *Final project report: PSERC publication*, 2006.

[14] A. Kulkarni, A Hidden Reliability Threat in UPS Static Bypass Switches, *Schneider Electric white paper library*, 2011.

[15] Schaefer Engineering, Static Switches, Available online: www.schaeferpower.com.

[16] Standard EN 50160-2004, Voltage Characteristics in Public Distribution Systems, *Brussels, Belgium*, 2004.

[17] Technical requirements for connecting distributed recourses to the Manitoba Hydro system, *Manitoba Hydro-Electric Board, DRG 2003, Rev2*, 2011.

[18] G. Gurrala, I. Sen, "Power System Stabilizers Design for Interconnected Power Systems," *IEEE Trans. Power Syst*, vol. 25, pp. 1042-1051, 2010.

[19] X.F. Wang, Y. Song, M. Irving, *Modern Power Systems Analysis*, New York: Springer-Verlag, 2009.

[20] D. Ketata, L. Krichen, "Modeling, control, and power management of a power electrical system including two distributed generators based on fuel cell and supercapacitor," *Renew. Sustainable Energy*, vol. 5, pp. 033122-033137, 2013.

[21] F. Bensmaine, A. Barakat, S. Tnani, G. Champenois, E. Mouni, "Dual control of synchronous generator for terminal voltage regulation-comparison with a single control," *Electr. Power Syst. Res*, vol. 91, pp. 78-86, 2012.

[22] A. Kumar Jain, V. T. Ranganathan, "Modeling and Field Oriented Control of Salient Pole Wound Field Synchronous Machine in Stator Flux Coordinates," *IEEE Trans. Industrial* Electronics, vol. 58, pp. 960-970 , 2011.

[23] A. Barakat, S. Tnani, G. Champenois, E. Mouni, "Analysis of synchronous machine modeling for simulation and industrial applications," *Simul. Model. Pract. Th*, vol. 18, pp. 1382-1396, 2010.

[24] A.M. El-Zonkoly, "Optimal placement of multi-distributed generation units including different load models using particle swarm optimization," *Swarm and Evolutionary Computation*, vol. 1, pp. 50-59, 2011.

[25] B. DeMetz-Noblat, G. Jeanjean, Dynamic stability of industrial electrical networks, *Technical collection no. 185, Schneider Electric*, 1997.

[26] R. Kallel, G. Boukettaya, L. Krichen, "Control Management Strategy of Stand-Alone Hybrid Power Micro-System using Super-Capacitor," *International Journal of Renewable Energy Research*, vol. 4, pp. 210-223, 2014.

[27] M. Dicorato, G. Forte, M. Trovato, "Wind farm stability analysis in the presence of variable-speed generators," *Energy*, vol. 39, pp. 40-47, 2012.

[28] H.W. Kim, S.S. Kim, H.S. Ko, "Modeling and control of PMSG-based variable-speed wind turbine," *Electr. Power Syst. Res*, vol. 80, pp. 46-52, 2010.

[29] A. Kusiak, H. Zheng, Z. Song, "Short-term prediction of wind farm power: A data mining approach," *IEEE Trans. Energy Convers*, vol. 24, pp. 125-136, 2009.

[30] L.C. Cradden, F. Restuccia, S.L. Hawkins, G.P. Harrison, "Consideration of Wind Speed Variability in Creating a Regional Aggregate Wind Power Time Series," *Resources*, vol. 3, pp. 215-234, 2014.

[31] M. Rekik, A. Abdelkafi; L. Krichen, "A novel control strategy of a distributed generator operating in seven modes for ancillary services under grid faults," *Elec. Power Energy Syst*, vol. 47, pp. 100-108, 2013.

[32] M.A. Tankari, M.B. Camara, B. Dakyo, C. Nichita, "Ultracapacitors and Batteries Integration for Power Fluctuations mitigation in Wind-PV-Diesel Hybrid System," *International Journal of Renewable Energy Research*, vol. 1, pp. 86-95, 2011.

Nomenclature

WRSG	Wound Rotor Synchronous Generator	v	wind speed
Te	WRSG electromagnetic torque	R	blade radius
T_m	WRSG mechanical torque	Ω_t	blades rotational speed
ϕ_d, ϕ_q	direct and transverse stator leakage flux of the WRSG	C_p	power coefficient
ω_{ep}	electrical angular speed of the WRSG	S	wind turbine swept area
Ω_{ep}	rotor mechanical speed of the WRSG	ρ	air density
V_d, V_q	direct and transverse output voltages of the WRSG	λ	tip speed ratio
i_d, i_q	direct and transverse armature currents of the WRSG	PMSG	Permanent Magnet Synchronous Generator
i_D, i_Q	direct and transverse dampers currents of the WRSG	C_{em}	PMSG electromagnetic torque
V_f	main field excitation voltage of the WRSG	C_m	PMSG mechanical torque
i_f	main field excitation current of the WRSG	J	rotor and turbine inertia
r_s	stator resistance of the WRSG	Ω	rotor mechanical speed of the PMSG
l_d, l_q	d-q stator main inductances of the WRSG	V_{sd}, V_{sq}	d-q components of the PMSG stator voltages
r_D, r_Q	dampers resistances of the WRSG	ϕ_m	PMSG stator flux
l_D, l_Q	d-q dampers inductances of the WRSG	L_d, L_q	d-q components of the stator winding inductance of the PMSG
r_f	main field resistance	R_s	stator winding resistance of the PMSG
l_f	main field inductance	p	number of pole pairs of the PMSG
M_{sf}	mutual inductance between direct stator winding and main field	R_{fi}	filter resistance
M_{sD}	mutual inductance between stator and direct damper	L_{fi}	filter inductance
M_{sQ}	mutual inductance between the stator and quadrature damper	C_{fi}	filter capacitance
M_{fD}	mutual inductance between the main field winding and direct damper	U_{bus}	DC bus voltage
n_p	number of pole pairs of the WRSG	C_{bus}	DC bus capacitance